

REVISION 1

American Mineralogist

LETTER

The glass transition temperature of anhydrous amorphous calcium carbonate

Word count: 1747

Thilo Bissbort¹, Kai-Uwe Hess¹, Martin Wilding², Jürgen E. K. Schawe^{3,4}, Bettina Purgstaller⁵,
Katja E. Goetschl⁵, Sebastian Sturm⁶, Knut Müller-Caspary⁶, Elena V. Sturm¹, Wolfgang
Schmahl¹, Erika Griesshaber¹, Daniel Weidendorfer¹, Martin Dietzel⁵, Donald B. Dingwell¹

¹*Earth and Environmental Sciences, Ludwig-Maximilians-Universität München, Theresienstraße 41/III,
80333 München, Germany*

²*UK Catalysis Hub, Research Complex at Harwell, Rutherford Appleton Laboratory, Harwell Campus,
Oxfordshire OX11 0FA, United Kingdom*

³*Mettler-Toledo GmbH, Heuwinkelstrasse 3, CH-8603, Nänikon, Switzerland*

⁴*Laboratory of Metal Physics and Technology, Department of Materials, ETH Zurich, 8093 Zurich,
Switzerland*

⁵*Institute of Applied Geosciences, Graz University of Technology, Rechbauerstrasse 12, 8010 Graz,
Austria*

⁶*Fakultät für Chemie und Pharmazie, Physikalische Chemie, Ludwig-Maximilians-Universität München,
Butenandstr. 5-13, 81377, München, Germany*

* Corresponding author: Thilo Bissbort

24 **Email:** thilo.bissbort@lmu.de

25 **Abstract**

26 Amorphous calcium carbonate (ACC) is the least stable polymorph of calcium
27 carbonates. It has been identified to play an important role in nature (e.g.,
28 biomineralization and speleothem formation), where it acts as a precursor for the
29 transformation to more stable polymorphs such as calcite. Further, the use of ACC in
30 technical applications requires a robust understanding of the material's properties. We
31 present the first study that reveals the existence of a glass transition for synthetic and
32 anhydrous ACC. The glass transition occurs at 339 °C. Such measurements are
33 impossible with conventional differential scanning calorimetry (DSC) due to the high
34 tendency of ACC to crystallize. Fast scanning DSC with heating rates of 500 °C/s and
35 higher, however, can be used to separate the endothermic glass transition signature from
36 the exothermic crystallization event since crystallization is shifted to higher temperatures.
37 This allows the detection and quantification of the glass transition for ACC. These
38 observations indicate that ACC is a structural glass and is especially significant because
39 the synthesis of ACC, precipitation from a solution followed by lyophilization, contrasts
40 with the more conventional and well-known route of glass formation the rapid cooling of
41 a melt. Moreover, we prove that a structural glass can be produced from a simple single-
42 component carbonate system.

43

44 **Keywords:** glass transition temperature – amorphous calcium carbonate – flash
45 differential scanning calorimetry - lyophilization

46 **Introduction**

47

48 Amorphous calcium carbonate (ACC), $\text{CaCO}_3 \cdot n\text{H}_2\text{O}$, is a naturally occurring, although
49 unstable form of calcium carbonate and has been recognized as playing an important role
50 in biomineralization processes. Since its discovery (Sturcke 1898), it has been the subject
51 of particular interest since, aside from its role in biogenesis there are further technical
52 applications in, for example pharmaceuticals and in CO_2 sequestration, e.g., Politi et al.
53 (2004). Despite this, the characteristic properties of ACC and the formation process are
54 not well understood. ACC is the least stable form of calcium carbonate and has been
55 shown to exist in hydrous and anhydrous forms. Anhydrous ACC can be transformed to
56 more stable polymorphs of calcium carbonate such as vaterite, aragonite and ultimately
57 calcite by the progressive reduction of enthalpy (Radha et al. 2010).

58

59 Amorphous solids show no long-range order identified e.g., by the lack of Bragg
60 reflections in wide-angle X-ray or electron diffraction. Tammann (1903) proposed the
61 “classical” method to produce amorphous glassy materials to bypass the crystallization
62 by rapidly cooling a melt below the glass transition. Further techniques are used to make
63 a glass e.g., spray drying or lyophilization. For the definition of a glass we follow C.A.
64 Angell: “A (structural) glass is an amorphous solid, which is capable of passing
65 continuously into the viscous liquid state, usually, but not necessarily, accompanied by an
66 abrupt increase in heat capacity” (Angell 2004). Therefore, the observation of a glass
67 transition in ACC implies that it is a structural glass.

68

Usually, the glass transition (i.e., an abrupt change in heat capacity), can be identified by differential scanning calorimetry (DSC). In the case of rapidly crystallizing materials like ACC, the glass transition may be completely superimposed by the exothermal crystallization peak. Such crystallization peak has been measured in ACC between 320 and 330 °C and no glass transition (i.e., endothermal peak) was observed (Koga et al. 1998; Koga and Yamane 2008; Wolf and Günther 2001; Radha et al. 2010). However, the higher heating rate dependence of crystallization, compared to that of glass transition, provides a way to separate the two processes at sufficiently high heating rates (Schawe and Löffler 2019). Thus, we use the fast-scanning calorimetry to identify and quantify the glass transition of ACC. A classification of ACC as a structural glass, although synthesized in the laboratory under controlled conditions in this study, will further deepen our understanding of its role in natural applications such as biomineralization and carbonate melts.

Materials and Methods

Synthesis

Hydrous amorphous calcium carbonate (ACC: $\text{CaCO}_3 \cdot n\text{H}_2\text{O}$) was synthesized by mixing the two solutions 0.25M CaCl_2 and 0.25M Na_2CO_3 produced from $\text{CaCl}_2 \cdot 2\text{H}_2\text{O}$, Na_2CO_3 (Carl Roth Chemicals) and ultrapure deionized water (DW: $18.2 \text{ M}\Omega \text{ cm}^{-1}$). The solutions were kept in a refrigerator at 10 ± 1 °C for at least 4 hours prior to mixing. The precipitated ACC was separated using a 0.2 μm cellulose filter and a suction filtration device and rinsed twice with pre-cooled DW to remove Na^+ and Cl^- ions. Instantaneously

92 after filtration, the separated ACC was freeze-dried for 12 hours in a Virtis Benchtop 3L
93 and subsequently stored in a desiccator at ambient temperature using silica gel as drying
94 agent.

95

96 ***Transmission Electron Microscopy***

97

98 A probe-corrected FEI Themis microscope operated at an acceleration voltage of 300 kV
99 and equipped with a SuperXG1 EDX detector was used to obtain high-angle annular
100 dark-field scanning transmission electron microscopy (HAADF-STEM) images, electron
101 diffraction patterns, energy-dispersive X-ray (EDX) spectra and elemental mappings of
102 powder sample of freeze-dried ACC which was deposited onto 2 nm carbon-coated TEM
103 grid (QUANTIFOIL®). The data were analyzed with the software DigitalMicrograph®
104 (Gatan) and Velox (ThermoFisher Scientific).

105

106 ***Thermal gravimetry and conventional DSC***

107

108 Thermal gravimetry combined with conventional DSC was performed at heating rates of
109 10 °C/min using a Netzsch STA 449 F1. Samples of 3 to 5 mg of freeze-dried ACC and
110 ACC further dried at 250 °C (anhydrous ACC) were heated in Pt-crucibles with a lid up
111 to 350 °C. These measurements were performed in a high purity argon atmosphere with
112 flow rates of 100 ml/min.

113

Fast scanning differential scanning calorimetry (FDSC)

The Flash DSC 2+ (Mettler-Toledo), which was used with a UFS1 calorimeter chip (van Herwaarden et al. 2011). This sensor provides typical maximum heating and cooling rates of 40,000 °C/s and 4,000 °C/s, respectively. Due to the low heat conductivity of ACC we use heating and cooling rates up to 2000 °C/s to minimize effects of thermal inertia. The sample side of the sensors were coated with a thin layer of silicon oil (AK 500.000 Wacker) to improve the thermal contact between sensor and samples with irregular shape (Koulialias et al. 2021). The temperature program consisted of an initial isothermal segment at 250 °C of 10 min followed by four heating-cooling cycles with matching heating and cooling rates. ACC crystallized upon cooling after the first heating, even though heating was terminated right after the glass transition was observed and before crystallization during heating occurred. The three heating curves of the crystallized material were used as baseline. All FDSC measurements were performed in a CO₂ flow of 30 mL/min. The glass transition temperature is defined as thermodynamic glass transition temperature (Richardson and Savill 1975) or the limiting fictive temperature (Moynihan et al. 1976). Both definitions equally quantify T_g by the integral technique.

Results

The morphology and size of freeze-dried ACC was characterized by HAADF-STEM. The acquired images reveal that ACC exists as polydisperse spheres with diameters between 10 and 150 nm, which form random aggregates (Figure 1A). Compositional

homogeneity was verified by EDXS. High resolution HAADF-STEM images lack any signs of crystallinity, thus confirming the amorphous structure of ACC (Figure 1B). Weight loss curves obtained by heating from ambient temperature to 350 °C using STA (a combination of thermal gravimetry (TGA) and conventional differential scanning calorimetry (DSC)) indicate that the original ACC material (freeze-dried) contains 6.89 ± 0.1 wt% water (0.411 mole H₂O per mole ACC) (Figure 2). No further weight loss is observed for material that has been dried at 250 °C (anhydrous ACC).

We performed calorimetric measurements to determine the glass transition temperature, T_g , of anhydrous ACC using FDSC. ACC is hydrous after synthesis, see above. To obtain anhydrous ACC, samples were further dried at 250 °C for 10 min in CO₂ directly in the FDSC device. At these conditions no crystallization and further mass loss was observed, as proven by STA. FDSC measurements were performed during heating with 500, 1000, 1500, and 2000 °C/s (Figure 3A). Glass transition and crystallization separate clearly at these rates. The glass transition temperature, T_g , seems to increase with increasing heating rate (Figure 3B). The reason is the influence of thermal inertia on the measurement curves. This behavior is described by equation 1 (Schawe 2007).

$$T_g = T_{g0} + \beta\tau(1 - \exp(-\frac{\Delta T}{2\beta\tau})) \quad (1)$$

where T_g is the measured glass transition temperature at a specific heating rate, T_{g0} is the glass transition temperature corrected by the thermal inertia, β is the heating rate, τ is the effective thermal lag of sensor and sample, and ΔT is the width of the glass transition.

157 The resulting effective thermal lag is 16 ms, ΔT is 54 °C, and the glass transition
158 temperature of synthetic anhydrous ACC is $T_{g0} = 339$ °C.

159

160 **Discussion**

161

162 Synthetic anhydrous ACC undergoes a stepwise increase in heat capacity while crossing
163 the glass transition. This is a clear indication for a structural glass, although it was
164 produced by precipitation from a solution followed by lyophilization. Recently, Hess et
165 al. (2023) have demonstrated the glass-forming abilities for a binary carbonatitic system
166 (amorphous calcium-magnesium carbonate, APMC). Here, we have shown for the first
167 time that a single component carbonate system (calcium carbonate), can form glass
168 following the same synthesis procedure. Compared to ACC with a T_g of 339 °C, APMC
169 exhibits “higher” glass transition temperatures at all heating rates with a heating-rate-
170 independent glass transition temperature of 376 °C. This suggests that the substitution of
171 Ca by Mg in ACC increases the glass transition temperature. Since APMC is more stable
172 than ACC, it was previously possible to study the amorphous two-component carbonate.

173 **Implications**

174

175 Our study shows that a material that was thought to be an amorphous solid is a structural
176 glass. The observation of a glass transition for anhydrous ACC was only possible by
177 applying very fast heating rates. It is therefore reasonable to assume that the same is true
178 for other amorphous materials. For such materials, then, the separation between

179 amorphous solids and glasses is meaningless and the limiting fictive temperature could be
180 used as a general order parameter to describe the solid amorphous state in the sense of
181 Gupta and Moynihan (1976). However, to characterize the kinetics of the glass transition,
182 it is necessary to determine its cooling rate dependence. This has not been achieved so
183 far. Our study expands the still very limited knowledge about glass transitions of
184 carbonate systems that are of petrological relevance (cf. Weidendorfer et al. (2023) and
185 Hess et al. (2023)). This may provide important implications for carbonate phases in
186 subsurface environments (e.g., biomineralization or magmatic processes). The fact that an
187 amorphous solid that is formed through lyophilization can be a structural glass, i.e., it is
188 formed by crossing a glass transition, implies that the materials properties change
189 drastically while crossing this boundary, which will finally affect the material's
190 macroscopic behavior in natural and anthropogenic applications.

191 **Acknowledgments** 192

193 The synthesis of ACC was conducted at NAWI Graz Central Lab of Water Minerals and
194 Rocks (NAWI Graz Geocentre, Austria). DBD acknowledges the support of the
195 European Research Council (ERC) 2018 AdG Grant 834255 „EAVESDROP”. We thank
196 the anonymous reviewer for their comments and Yann Morizet for editorial handling.

197
198 **Author Contributions:** TB, KUH, MW, JEKS: conceptualization, methodology,
199 investigation, writing; BP, KEG, SS, KMC, EVS, WS, EG, DW: methodology,
200 investigation, writing; MD, DBD: writing.

201

202 **Competing Interest Statement:** The authors declare no competing interest.

203

204

205 REFERENCES CITED

- 206 Angell, C.A. (2004) Encyclopedia of Materials: Science and Technology, 1–11.
207 Hess, K.-U., Schawe, J.E.K., Wilding, M., Purgstaller, B., Goetschl, K.E., Sturm, S.,
208 Müller-Caspary, K., Sturm, E.V., Schmahl, W., Griesshaber, E., Bissbort, T.,
209 Weidendorfer, D., Dietzel, M., and Dingwell, D.B. (2023) Glass transition
210 temperatures and crystallization kinetics of a synthetic, anhydrous, amorphous
211 calcium-magnesium carbonate. Philosophical transactions. Series A, Mathematical,
212 physical, and engineering sciences, 381 (2258), 20220356, DOI:
213 10.1098/rsta.2022.0356 (eng).
214 Koga, N., and Yamane, Y. (2008) Thermal behaviors of amorphous calcium carbonates
215 prepared in aqueous and ethanol media. Journal of Thermal Analysis and Calorimetry,
216 94 (2), 379–387, DOI: 10.1007/s10973-008-9110-3 (En;en).
217 Koga, N., Nakagoe, Y., and Tanaka, H. (1998) Crystallization of amorphous calcium
218 carbonate. Thermochimica Acta, 318 (1-2), 239–244, DOI: 10.1016/S0040-
219 6031(98)00348-7.
220 Koulialias, D., Schawe, J.E.K., Löffler, J.F., and Gehring, A.U. (2021) Structural
221 relaxation in layered, non-stoichiometric Fe₇S₈. Physical chemistry chemical physics :
222 PCCP, 23 (2), 1165–1171, DOI: 10.1039/d0cp04445h (eng).
223 Moynihan, C.T., Easteal, A.J., Bolt, M.A., and Tucker, J. (1976) Dependence of the
224 Fictive Temperature of Glass on Cooling Rate. Journal of the American Ceramic
225 Society, 59 (1-2), 12–16, DOI: 10.1111/j.1151-2916.1976.tb09376.x.
226 Politi, Y., Arad, T., Klein, E., Weiner, S., and Addadi, L. (2004) Sea urchin spine calcite
227 forms via a transient amorphous calcium carbonate phase. Science, 306 (5699), 1161–
228 1164, DOI: 10.1126/science.1102289 (eng).
229 Radha, A.V., Forbes, T.Z., Killian, C.E., Gilbert, P.U.P.A., and Navrotsky, A. (2010)
230 Transformation and crystallization energetics of synthetic and biogenic amorphous
231 calcium carbonate. Proceedings of the National Academy of Sciences of the United
232 States of America, 107 (38), 16438–16443, DOI: 10.1073/pnas.1009959107 (eng).
233 Richardson, M.J., and Savill, N.G. (1975) Derivation of accurate glass transition
234 temperatures by differential scanning calorimetry. Polymer, 16 (10), 753–757, DOI:
235 10.1016/0032-3861(75)90194-9.
236 Schawe, J.E.K. (2007) An analysis of the meta stable structure of poly(ethylene
237 terephthalate) by conventional DSC. Thermochimica Acta, 461 (1-2), 145–152, DOI:
238 10.1016/j.tca.2007.05.017.

- Schawe, J.E.K., and Löffler, J.F. (2019) Existence of multiple critical cooling rates which generate different types of monolithic metallic glass. *Nature Communications*, 10 (1), 1337, DOI: 10.1038/s41467-018-07930-3 (eng).
- Sturcke, H.E. (1898) Process of preparing amorphous carbonate of lime from residues (US603225A).
- Tammann, G. (1903) *Kristallisieren und Schmelzen: ein Beitrag zur Lehre der Änderungen des Aggregatzustandes*. J.A. Barth, Leipzig.
- van Herwaarden, S., Iervolino, E., van Herwaarden, F., Wijffels, T., Leenaers, A., and Mathot, V. (2011) Design, performance and analysis of thermal lag of the UFS1 twin-calorimeter chip for fast scanning calorimetry using the Mettler-Toledo Flash DSC 1. *Thermochimica Acta*, 522 (1-2), 46–52, DOI: 10.1016/j.tca.2011.05.025.
- Weidendorfer, D., Hess, K.-U., Ruhekenya, R.M., Schawe, J.E.K., Wilding, M.C., and Dingwell, D.B. (2023) Effect of water on the glass transition of a potassium-magnesium carbonate melt. *Philosophical transactions. Series A, Mathematical, physical, and engineering sciences*, 381 (2258), 20220355, DOI: 10.1098/rsta.2022.0355 (eng).
- Wolf, G., and Günther, C. (2001) Thermophysical Investigations of the Polymorphous Phases of Calcium Carbonate. *Journal of Thermal Analysis and Calorimetry*, 65 (3), 687–698, DOI: 10.1023/A:1011991124181 (En;en).

Figure captions:

Figure 1: **A** – HAADF-STEM image of an aggregate of freeze-dried ACC. **B** – Magnification of a single ACC spherule of the aggregate shown in A. Signs of crystallinity are absent.

Figure 2: Results from TGA (black) and conventional DSC (blue) measurements for freeze-dried (dotted lines) ACC and ACC that has been dried at 250 °C (i.e., anhydrous). Heating rates were 10 °C/min.

270 **Figure 3: A** - Heat flow curves obtained during heating at rates of 500, 1000, 1500, and
271 2000 °C/s using FDSC. All curves exhibit the glass transition (T_g indicated by arrows)
272 before crystallization (intense exothermic peak). **B** - The glass transition temperatures
273 determined at different heating rates for ACC (black symbols). A correction for thermal
274 lag (equation 1, red line) provides the glass transition temperature of 339 °C, which is
275 independent of the heating rate. The glass transition temperature of synthetic anhydrous
276 ACC is lower than that of synthetic anhydrous APMC (Hess et al. 2023), which is 376
277 °C (grey symbol and line). Note, only one datapoint for APMC is shown, since the other
278 measurements of APMC were performed at higher heating rates of up to 6000 °C/s.

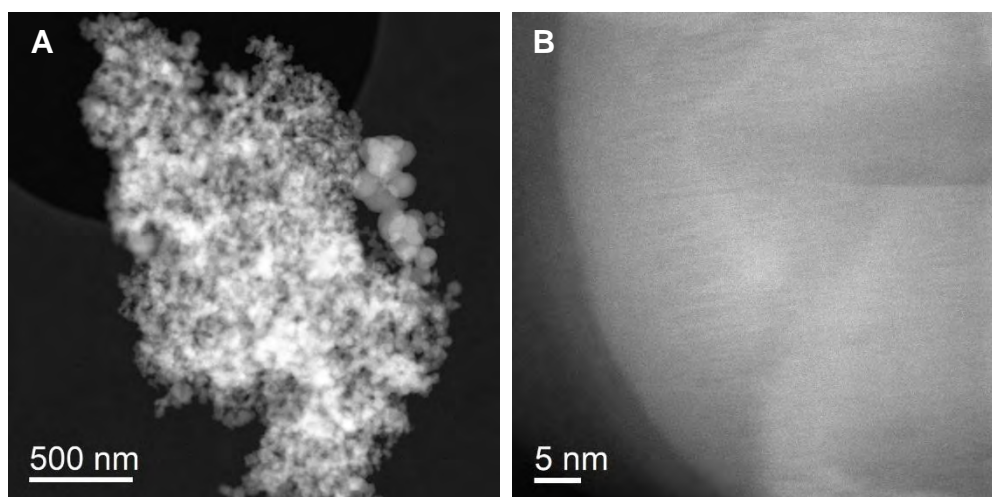


Figure 1

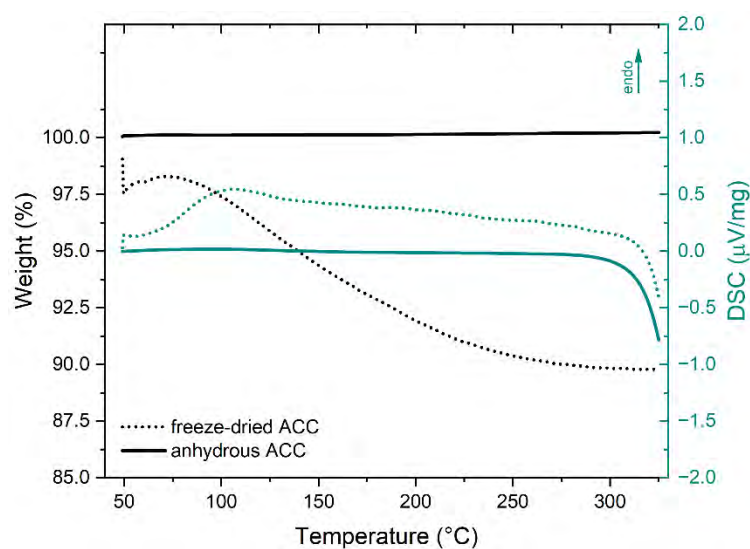


Figure 2

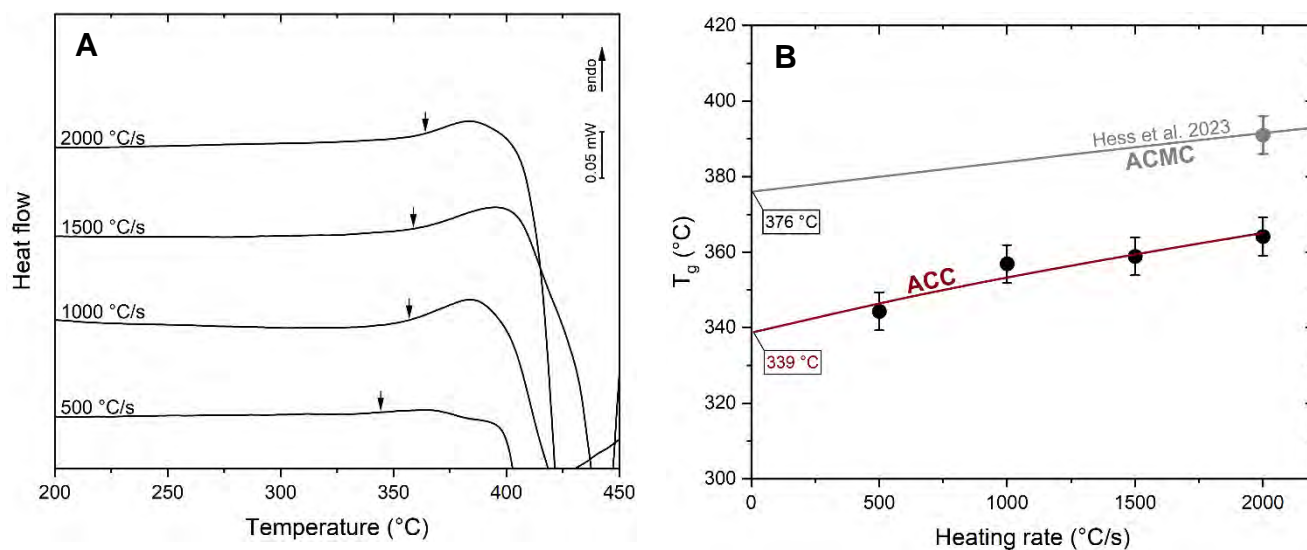


Figure 3

288